Influence of magnetocrystalline anisotropy on the magnetization dynamics of magnetic microstructures

2009 J. Phys.: Condens. Matter 21 314008

(http://iopscience.iop.org/0953-8984/21/31/314008)

J. Phys.: Condens. Matter **21** (2009) 314008 (6pp) doi:10.1088/0953-8984/21/31/314008

Influence of magnetocrystalline anisotropy on the magnetization dynamics of magnetic microstructures

A Kaiser, C Wiemann, S Cramm and C M Schneider

Forschungszentrum Jülich, Institut für Festkörperforschung IFF-9, and JARA-FIT, 52425 Jülich, Germany

E-mail: a.kaiser@fz-juelich.de

Received 29 December 2008, in final form 12 February 2009
Published 7 July 2009
Online at stacks.iop.org/JPhysCM/21/314008

Abstract

The study of magnetodynamics using stroboscopic time-resolved x-ray photoemission electron microscopy (TR-XPEEM) involves an intrinsic timescale provided by the pulse structure of the synchrotron radiation. In the usual multi-bunch operation mode, the time span between two subsequent light pulses is too short to allow a relaxation of the system into the ground state before the next pump–probe cycle starts. Using a deflection gating mechanism described in this paper we are able to pick the photoemission signal resulting from selected light pulses. Thus, PEEM measurements can be carried out in a flexible timing scheme with longer delays between two light pulses. Using this technique, the magnetodynamics of both Permalloy and iron structures have been investigated. The differences in the dynamic response on a short magnetic field pulse are discussed with respect to the magnetocrystalline anisotropy.

(Some figures in this article are in colour only in the electronic version)

1. Introduction

During the last 15 years x-ray photoemission electron microscopy (XPEEM) using synchrotron radiation has matured into a well-established tool for element-selective imaging of magnetic domains and the study of complex magnetic systems [1–3]. By illumination with circularly polarized light a magnetic contrast from a ferromagnetically ordered state is generated due to the x-ray magnetic circular dichroism (XMCD) [4]. The magnetic contribution to the signal I_{mag} depends on the relative orientation between the light helicity vector $\mathbf{q}$ and local magnetization direction $\mathbf{M}$:

$$I_{\mathrm{mag}} \propto \mathbf{q} \cdot \mathbf{M}.$$

When the light helicity is reversed, the sign of the magnetic contrast is inverted, too, whereas contrast contributions from the surface topography or a lateral variation of the surface chemistry remain unaffected. Thus, by acquiring images for right (σ^+) and left (σ^-) circularly polarized light and calculating the XMCD asymmetry A_{XMCD}, the non-magnetic contributions may be removed:

$$I_{\mathrm{mag}} \propto A_{\mathrm{XMCD}} = \frac{I_{\sigma^+} - I_{\sigma^-}}{I_{\sigma^+} + I_{\sigma^-}}.$$

This image processing is usually performed on a pixel-by-pixel basis and in this way a contrast-enhanced image of the local magnetization is created. By tuning the photon energy to the absorption edges of different chemical constituents of the system, magnetic domains can be imaged in an element-selective manner [3].

By exploiting the intrinsic time structure of the synchrotron radiation—generated by the electron bunches circulating in the storage ring—time-resolved imaging of reversible magnetodynamic processes becomes possible using a pump–probe approach [5, 6]. The time resolution of such stroboscopic XPEEM experiments is limited by the width of the photon pulses to about 50–100 ps. For such experiments the sample has to be equipped with a coplanar waveguide into which short current pulses are injected, generating an Oersted field pulse (*pump*), which acts on the magnetic structures lithographically defined on top of the waveguide (see figure 1(a) for a schematic view). The pulse generator has to be synchronized to the repetition frequency of the

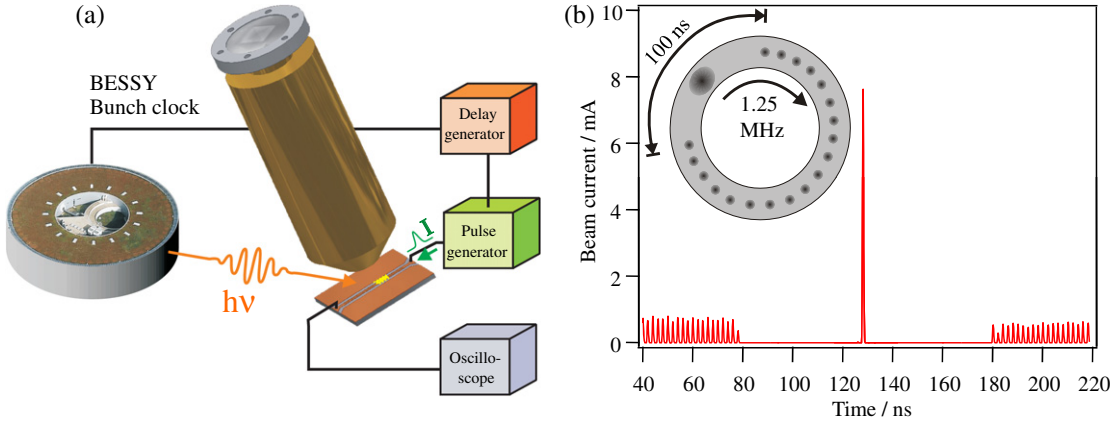

Figure 1. (a) Schematic view of the time-resolved PEEM experiment. (b) Bunch pattern in the BESSY hybrid bunch mode.

synchrotron x-ray pulses (at BESSY-II 500 MHz in multi-bunch mode and 1.25 MHz in single-bunch mode) to ensure that always the same micromagnetic state after the magnetic excitation is imaged by the light pulse (*probe*). By varying the delay between this pump–probe sequence consisting of magnetic excitation and synchrotron light illumination, entire image series of the magnetization dynamics mapping the time evolution of resonant precessions [7], vortex motion [8] and transient changes in the domain configuration [9] can be acquired.

In order to obtain a good signal-to-noise ratio, the images are generated by integrating over several million pump–probe cycles. Therefore the time between subsequent pump–probe cycles must be such that the magnetic system can relax to a defined ground state, before the next pump is initiated by injecting a current pulse through the waveguide. Otherwise ill-defined intermediate states may be probed. In most of the magnetodynamic processes of interest relaxation takes place on a much slower timescale than the excitation process. This is partially due to the fact that the restoring force or torque acting on the magnetic system after the decay of the field pulse is often provided only by the demagnetizing field. With most synchrotrons working with a typical bunch repetition frequency of 500 MHz, the delay between two subsequent light pulses is only 2 ns, which is usually much smaller than the required relaxation time of 10–20 ns, for example, if domain wall motion is involved. Due to this reason special operation modes where only one or a few widely separated electron bunches are circulating inside the storage ring have to be used for the investigation of magnetodynamic processes. As an alternative, gating mechanisms have to be developed to suppress the contribution of unwanted light bunches. At many light sources hybrid bunch modes are provided in which most of the intensity is carried by several hundred small electron packets ('multi-bunches') following each other with 2 ns temporal separation (values valid for BESSY-II, Berlin) and one larger bunch ('single-bunch') which is isolated from the other bunches by a gap around 100 ns wide (see figure 1(b)). Using suitable gating mechanisms one can suppress the contribution of the smaller multi-bunches to the PEEM image generation and only use the isolated single-bunches, which have a repetition time of 800 ns at BESSY-II.

2. Experimental details

The experiments have been carried out using a modified FOCUS IS-PEEM, which is equipped with a quadrupole deflector system mounted close to the iris aperture (see sketch of beam path in figure 2(a)). The contrast aperture has been moved into a focal plane behind the iris aperture. By applying a short voltage pulse to the deflector electrodes in the x- or y-direction the photoelectron beam can be switched between passing through the contrast aperture (ON state) and being blocked by it (OFF state) within a time interval of 20 ns. The gating electronics driving the deflection is synchronized to the storage ring's repetition frequency. A schematic drawing is shown in figure 2(b) and a detailed description of the gating mechanism will be given elsewhere [10].

The change of deflection voltage yields a movement of the photoelectron beam relative to the contrast aperture. By small shifts of the contrast aperture the angular distribution of the selected photoelectrons is slightly changed. When the shift is small compared to the diameter of the contrast aperture the effect on the spatial resolution is negligible. In order to eliminate image deterioration due to gating, stable deflection voltages during the photoelectron pulses have to be ensured. In our experimental case, the gating voltage pulse is significantly longer than the temporal width of the photon bunch (20 ns compared to 50 ps) and the temporal jitter of the involved electronics is shorter than the bunch width (10 ps compared to 50 ps). Thus the voltage deflecting the hybrid bunch electrons can be assumed to be constant and the same photoelectron distribution is always passing the contrast aperture. The measured photoelectron distributions at both image and focal planes of the microscope have been compared with the non-gated case and no influence of the gating on the image quality except the reduction of intensity could be observed. However, it has to be noted that our microscope only has one projective lens and is thus not optimized for spatial resolution. A degradation of the spatial resolution in the 10 nm range cannot be detected.

The samples used for magnetodynamic measurements have been deposited by MBE onto GaAs substrates with a 200 nm thick Ag buffer layer. By optical lithography and

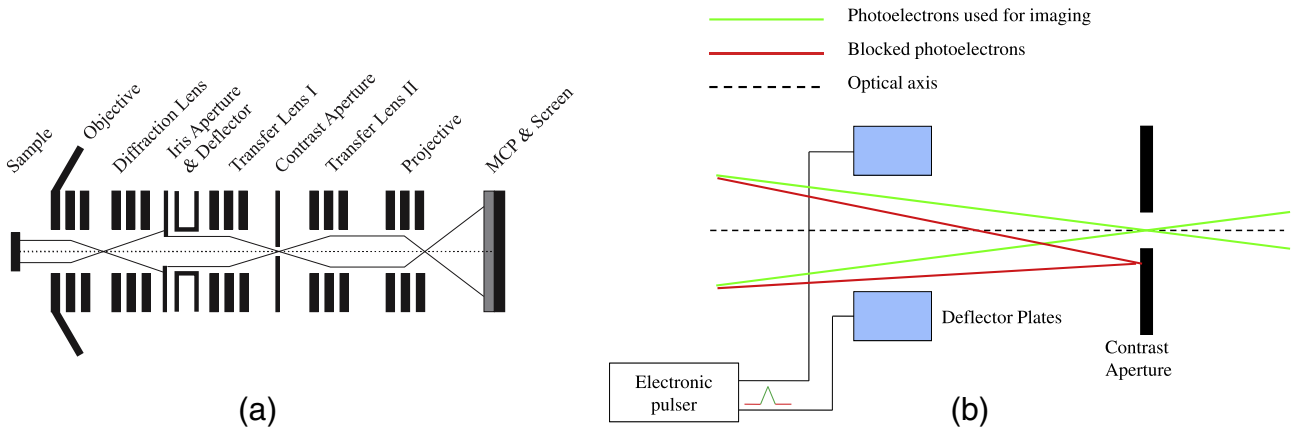

Figure 2. (a) Beam path in the PEEM and (b) a schematic drawing of the deflection gating technique.

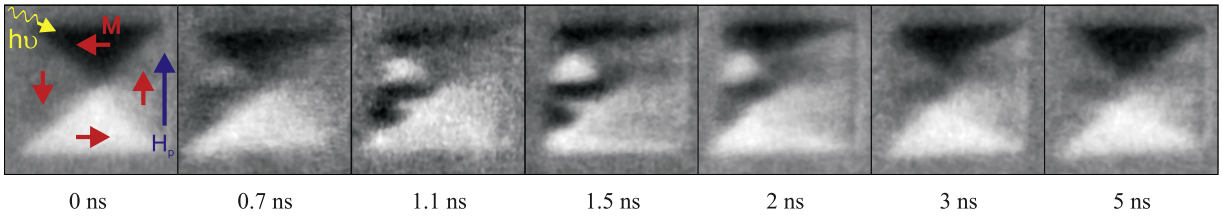

Figure 3. Pictures of the domain patterns in a 10 × 10 μm^2 Permalloy structure at different delays after magnetic field pulse excitation. The directions of the local magnetization and the external field are marked with arrows labelled with M and H_p.

Ar ion beam milling, coplanar Ag-waveguides and micron sized magnetic structures on top of them have subsequently been defined. The measurements have been carried out at the variable polarization beamline UE56/1-SGM at BESSY-II (Berlin).

3. Magnetization dynamics studies

3.1. $Ni_{80}Fe_{20}$ microstructures

Using the deflection gating technique, we have investigated Permalloy ($Ni_{80}Fe_{20}$) and pure iron microstructures during multi-bunch operating conditions at BESSY-II. Figure 3 shows snapshots of the magnetization distribution in a 10 × 10 μm^2 Permalloy element taken at different time delays after the excitation by the magnetic field pulse. The images have been acquired with the photon energy tuned to the Fe-L_3 absorption edge. The magnetic pulse profile acting on the microstructure is shown in figure 4(a) (bottom). The Permalloy microstructure shows the characteristic micromagnetic response of a low-anisotropy material as known from previous experiments [9]. In the equilibrium ground state Landau flux-closure domain patterns are formed [11]. Due to the external field, the two domains with magnetization components perpendicular to the external field pulse (top and bottom) are subject to a torque and shortly after the onset of the pulse the local magnetization vector is rotated towards the direction of the external field $\mathbf{H}_p$. The domain on the right-hand side of the structure, which has its magnetization oriented parallel to the field pulse, is growing by moving its domain walls to the left, while in the domain on the left a characteristic stripe pattern is formed by incoherent rotation processes, decreasing the area with energetically unfavourable antiparallel orientation between magnetization $\mathbf{M}$ and magnetic field pulse $\mathbf{H}_p$. In ideal defect-free samples such stripe patterns would not be observed, since the domain antiparallel to the external magnetic field would experience no magnetic torque at all. The occurrence of such stripe patterns is attributed to an inhomogeneous magnetization distribution in the equilibrium state or structural imperfections [12]. Similar, but less pronounced stripe patterns are formed in the domain on the right during the trailing edge of the excitation pulse (t = 1.5–2 ns). The reason for this behaviour is the formation of a new transient equilibrium state in the presence of $\mathbf{H}_p$, as discussed in [9].

The temporal evolution of the XMCD signal integrated over areas in the two perpendicularly oriented domains (shown in the inset) is plotted in figure 4(a) (top). Both domains exhibit a rotation of the magnetization towards the magnetic field pulse during the rising edge of the pulse, decreasing the measured XMCD values. Shortly after the maximum of the external field has been reached, the system starts to relax back towards the Landau state. During the relaxation process, additional oscillations of the magnetization are observed (marked by arrows), which can be explained by the excitation of precessional modes in the corresponding domains. The process of magnetization relaxation takes place on a slower timescale than the initial rotation towards the field, which is due to the formation of the above mentioned stripe patterns, also referred to as 'blocked patterns' [13]. Since neighbouring domains in such stripe patterns are dipolarly coupled to each

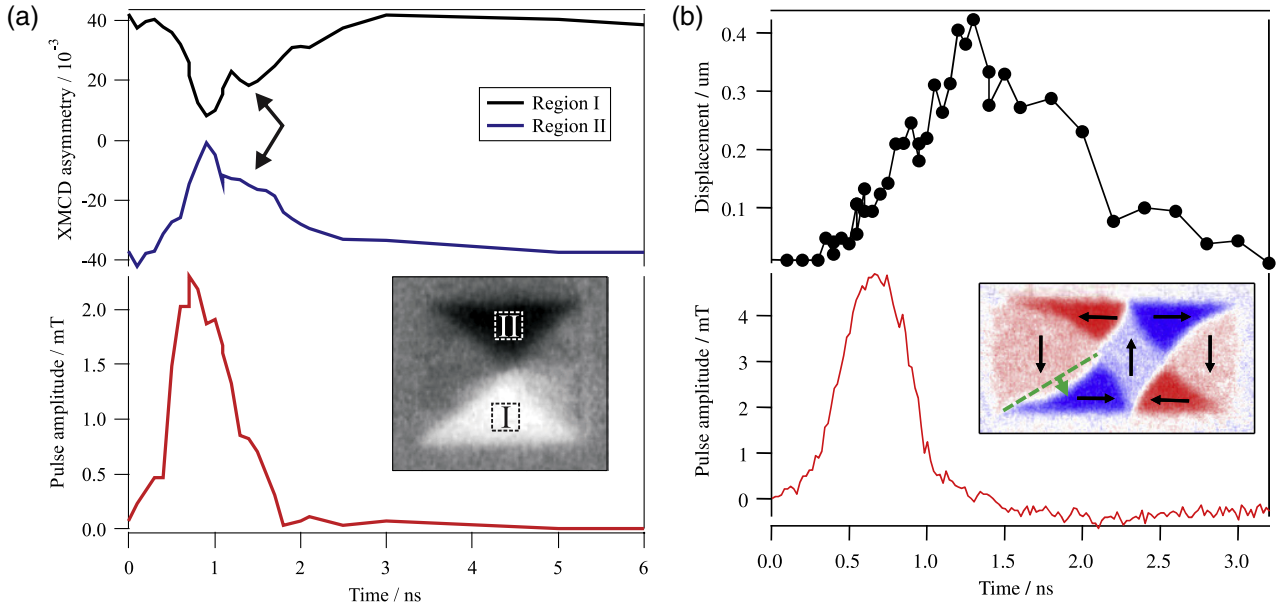

Figure 4. Temporal evolution of the magnetic structure as a response to the magnetic field pulse: (a) integrated XMCD signal in the two domains with $\mathbf{M} \perp \mathbf{H}_p$ (top) as a response on the magnetic field pulse (bottom). The relaxation of the magnetization rotation is superimposed by oscillations (marked by arrows) due to the excitation of magnetic eigenmodes. (b) Domain wall bulging in a $20 \times 10\ \mu m^2$ Fe element (inset) as a response to the magnetic field pulse (bottom).

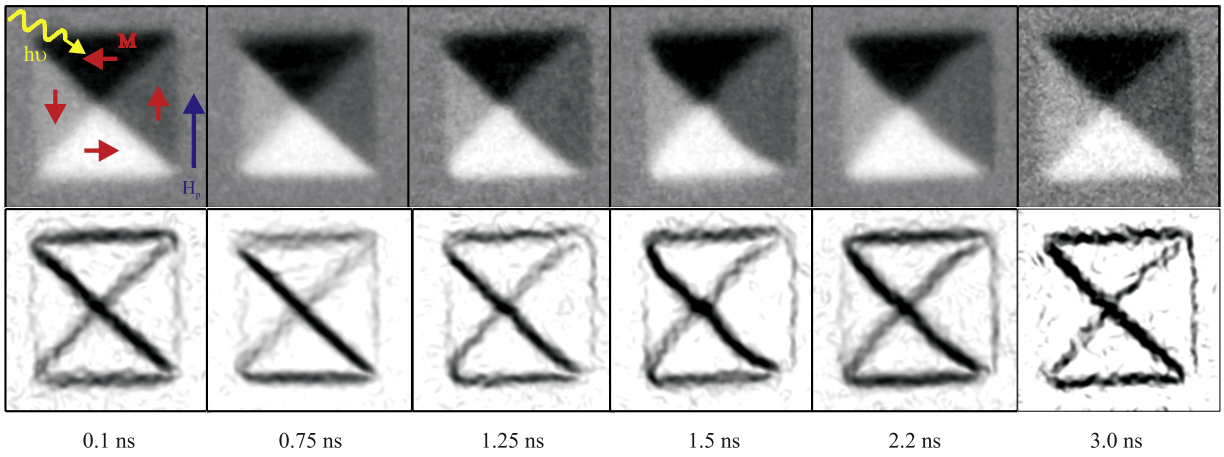

Figure 5. Images of the domain pattern in a $10 \times 10\ \mu m^2$ iron element as a function of time delay after magnetic excitation. The directions of the local magnetization and the external field pulse are marked with red and blue arrows. The pictures in the bottom row have been obtained by an edge detection algorithm in order to emphasize the position of the domain walls. The pictures for $t = 1.25$, 1.5 and 2.5 ns clearly show the bulging of the domain walls and a displacement of the vortex to the left.

other and separated by partial domain walls, they block themselves from relaxation into a mono-domain state, slowing down the process in the whole element.

3.2. Fe microstructures

Due to their epitaxial growth on single-crystalline Ag(001) buffer layers, Fe(001) films exhibit a strong four-fold in-plane magnetocrystalline anisotropy, which drastically affects the micromagnetic behaviour. Images of the magnetic domain pattern in the Fe element taken at different delay times after the magnetic excitation are compiled in figure 5. In the ground state, a Landau flux-closure pattern is observed consisting of four triangular domains parallel to the four easy axes of the iron film. No sizable rotation of the magnetization in any of these four domains is observed during or after the magnetic field pulse (figure 4(b), bottom). Instead, one observes a bulging of the domain walls and a displacement of the vortex core to the left (maximum at $t = 1.5$ ns). By this bulging and displacement effect the domain on the right-hand side with the local magnetization oriented parallel to the unipolar field pulse is growing at the expense of the domain with antiparallel magnetization components (left-hand side) and thus the magnetization integrated over the entire element develops a finite component into the pulse direction.

The reason for the difference in the magnetodynamic behaviour between the Permalloy and iron elements can be traced back to the different magnetocrystalline anisotropies in both materials. Since Permalloy exhibits virtually no magnetocrystalline anisotropy, the magnetization can freely rotate towards the external field. In epitaxial iron films the magnetization is strongly pinned along the four easy axes. Only if the Zeeman energy of the interaction between external field and magnetization is exceeding the anisotropy energy will the magnetization be turned out of the easy direction. In our experiments the peak magnetic field amplitude of 5 mT is not sufficient to achieve this and thus the main response to the magnetic field pulse is the domain wall motion leading to an increase of the magnetization component in the direction parallel to the pulse, integrated over the whole element.

Figure 4(b) shows the temporal evolution of the magnetic field pulse acting on the magnetic element (bottom) and the domain wall bulging in a $20 \times 10\ \mu\text{m}^2$ large Fe element (inset). For every image we have measured the displacement of the centre of the domain wall compared to a straight line between its end points (plotted in the top graph)—which represents the ground state. Starting with the onset of the field pulse, the domain wall centre begins to move with a constant speed of about 400 m s^{-1}, until the pulse has completely decayed. Then it relaxes with a lower speed of 200 m s^{-1} towards a straight line. During the relaxation process the temporal profile of the domain wall position is superimposed with an additional dip at around 2.0 ns. The maximum domain wall displacement is shifted with respect to the maximum excitation field by 700 ps.

We attribute the suppression of the higher amplitude precessional motion—as observed in the Permalloy case—as the reason for the rather long delay between the maxima of excitation and reaction. The Zeeman energy which is deposited by the external field into the spin system can only be consumed by the rather slow domain wall motion process, since coherent precession of the spins is mostly suppressed due to the magnetocrystalline anisotropy. Thus, the peak response is significantly delayed compared to other samples where precession is also an allowed energy dissipation channel.

We have simulated the micromagnetic behaviour of the iron elements using OOMMF [14]. All characteristic features of the measurements could be reproduced by the simulations. Moreover, the simulations predict a slight rotation of the magnetization vector **M** away from the easy axis by a maximum angle of 14°. This should give rise to a modulation of ∼3% in the XMCD signal. Such a minor change in the XMCD level cannot be resolved in our measurements due to the limited signal-to-noise ratio. A higher peak value of the field pulse in future experiments may increase this rotational response and may facilitate its experimental verification. The simulations also enable us to get a more detailed view on the domain wall bulging: we find that the maximum displacement of the domain wall is not statically located in its centre, but it is created near the edges of the wall and then moves along the domain wall.

Similar domain wall bulging effects have also been observed by Neudert *et al* [15]. They report an undulation of the domain walls in Permalloy elements in a quasistatic external field, which is explained by spatially modulated anisotropy in the polycrystalline sample. For our experiment, such a random-anisotropy effect can be ruled out: on the one hand the epitaxial growth of iron on the silver buffer layer clearly defines the magnetocrystalline axes of the material, on the other hand this effect would not have been reproduced in the simulations, since OOMMF assumes perfectly crystalline samples.

4. Conclusions

We have developed a novel gating technique for the realization of time-resolved XPEEM measurements in a 'virtual single-bunch mode' at BESSY-II. By this method we are able to extend the time span between two subsequent light pulses, which are used for imaging. This technique was applied to time-resolved XPEEM measurements on magnetic microstructures. We have carried out measurements on magnetically isotropic Permalloy elements and on iron elements exhibiting a strong four-fold in-plane anisotropy. Due to the differences in the magnetocrystalline anisotropy in both materials, we have observed a quite different micromagnetic behaviour in the response on a ns long magnetic field pulse. While the magnetization vector can freely rotate in Permalloy, in the iron film the domain magnetizations are pinned to the four easy axes, leading to a domain wall bulging in this material as the main response on the magnetic field pulse.

Acknowledgments

We thank H Pfeiffer for the development of the gating electronics, Dr K Grzelakowski for the electron-optical modifications and R Schreiber for sample preparation. This work was financially supported by the DFG (SFB 491) and the BMBF (05KS7UK1).

References

[1] Stöhr J, Wu Y, Hermsmeier B D, Samant M G, Harp G R, Koranda S, Dunham D and Tonner B P 1993 Element-specific magnetic microscopy with circularly polarized x-rays *Science* **259** 658

[2] Schönhense G 1999 Imaging of magnetic structures by photoemission electron microscopy *J. Phys.: Condens. Matter* **11** 9517

[3] Stöhr J and Anders S 2000 X-ray spectro-microscopy of complex materials and surfaces *IBM J. Res. Dev.* **44** 535

[4] Schütz G, Wagner W, Wilhelm W, Kienle P, Zeller R, Frahm R and Materlik G Feb 1987 Absorption of circularly polarized x rays in iron *Phys. Rev. Lett.* **58** 737

[5] Vogel J, Kuch W, Bonfim M, Camarero J, Pennec Y, Offi F, Fukumoto K, Kirschner J, Fontaine A and Pizzini S 2003 Time-resolved magnetic domain imaging by x-ray photoemission electron microscopy *Appl. Phys. Lett.* **82** 2299

[6] Schönhense G, Elmers H J, Nepijko S A and Schneider C M 2006 Time-resolved photoemission electron microscopy *Adv. Imag. Electron Phys.* **142** 159

[7] Krasyuk A, Wegelin F, Nepijko S A, Elmers H J, Schönhense G, Bolte M and Schneider CM 2005 Self-trapping of magnetic oscillation modes in Landau flux-closure structures *Phys. Rev. Lett.* **95** 207201

[8] Raabe J, Quitmann C, Back C H, Nolting F, Johnson S and Buehler C 2005 Quantitative analysis of magnetic excitations in Landau flux-closure structures using synchrotron-radiation microscopy *Phys. Rev. Lett.* **94** 217204

[9] Schneider C M *et al* 2004 Incoherent magnetization rotation observed in subnanosecond time-resolving x-ray photoemission electron microscopy *Appl. Phys. Lett.* **85** 2562

[10] Wiemann C, Kaiser A, Cramm S and Schneider C M 2009 Deflection gating for time-resolved XMCD-PEEM using synchrotron radiation *Rev. Sci. Instrum.* in preparation

[11] Hubert A and Schäfer R 1998 *Magnetic Domains—The Analysis of Magnetic Microstructures* (Berlin: Springer)

[12] Schönhense G, Elmers H J, Krasyuk A, Wegelin F, Nepijko S A, Oelsner A and Schneider C M 2006 Transient spatio-temporal domain patterns in permalloy microstructures induced by fast magnetic field pulses *Nucl. Instrum. Methods Phys. Res.* B **246** 1

[13] Chumakov D, McCord J, Schäfer R, Schultz L, Vinzelberg H, Kaltofen R and Mönch I 2005 Nanosecond time-scale switching of permalloy thin film elements studied by wide-field time-resolved Kerr microscopy *Phys. Rev.* B **71** 014410

[14] Donahue M J and Porter D G 1999 *OOMMF User's Guide, version 1.0, Interagency Report NISTIR 6376* National Institute of Standards and Technology

[15] Neudert A, McCord J, Chumakov D, Schäfer R and Schultz L 2005 Small-amplitude magnetization dynamics in permalloy elements investigated by time-resolved wide-field Kerr microscopy *Phys. Rev.* B **71** 134405